Int. J. Exp. Path. (2008), 89, 72–80
doi: 10.1111/j.1365-2613.2007.00564.x

ORIGINAL ARTICLE

Turbulent blood flow plays an essential localizing role in the development of atherosclerotic lesions in experimentally induced hypercholesterolaemia in rats

Cibele M. Prado*, Simone G. Ramos*, Jorge Elias Jr† and Marcos A. Rossi*

*Department of Pathology, Faculty of Medicine of Ribeirão Preto, University of São Paulo, Ribeirão Preto, SP, Brazil and
†Department of Internal Medicine, Faculty of Medicine of Ribeirão Preto, University of São Paulo, Ribeirão Preto, SP, Brazil

INTERNATIONAL JOURNAL OF EXPERIMENTAL PATHOLOGY

Summary

Taking into account that atherosclerosis is a focal disease and high levels of plasma cholesterol are closely correlated with its pathogenesis, it is a challenge to explain how equal concentrations of cholesterol bathing the endothelium can produce local, rather than global, effects on arteries. The focal distribution of atherosclerotic lesions has been considered to be dependent, at least in part, on hydrodynamic factors. The present study was carried out to further test the hypothesis that these forces are an important localizing factor in rats feeding a hypercholesterolaemic diet and submitted to infra-diaphragmatic aortic constriction. These animals develop a normotensive prestenotic region with laminar blood flow that serves as control for a normotensive poststenotic region with turbulent blood flow. Our findings clearly demonstrated that the combination of turbulent blood flow and low wall shear stress (WSS) in the presence of hypercholesterolaemia and oxidative stress creates conditions to the formation of focally distributed incipient atherosclerotic lesions observed in the poststenotic segment. In contrast, only diffuse fatty streaks could be observed in the normotensive prestenotic segment with laminar blood flow and normal WSS in the presence of hypercholesterolaemia and oxidative stress. Although haemodynamic forces are not by themselves responsible for the pathogenesis of atherosclerosis, they prime the local vascular wall in which the lesion develop. Further studies are required to establish how haemodynamic forces are detected and transduced into chemical signalling by the cells of the artery wall and then converted into pathophysiologically relevant phenotypic changes.

Keywords
atherosclerosis, hypercholesterolaemia, laminar blood flow, low wall shear stress, oxidative stress, turbulent blood flow

Received for publication:
21 August 2007
Accepted for publication:
7 September 2007

Correspondence:
Marcos A. Rossi, MD, PhD
Professor of Pathology
Department of Pathology
Faculty of Medicine of Ribeirão Preto
University of São Paulo
14049-900
Ribeirão Preto
SP, Brazil
Tel./Fax: +55 16 3602 3130
E-mail: marossi@fmrp.usp.br

The link between plasma levels of cholesterol and atherosclerosis was for the first time experimentally demonstrated in rabbits, almost a century ago, by Anitschkow and Chalatow (Anitschkow & Chalatow 1913). Since then, epidemiological (Anderson *et al.* 1987; Assmann *et al.* 2002), clinical trial (Klag *et al.* 1993; Grundy *et al.* 2004) and experimental data (Lichtman *et al.* 1999; Hartvigsen *et al.* 2007) have been demonstrating that high levels of plasma cholesterol are closely associated with the pathogenesis of atherosclerosis. Traditional theories on the pathophysiology of this relationship involve oxidized low-density lipoprotein (LDL) and deposition, modification, and cellular uptake of cholesterol and release of inflammatory and growth factors resulting in smooth muscle cell proliferation and collagen matrix production (Ross 1986; Steinberg *et al.* 1989). Taking into account that atherosclerosis is a focal disease, it is a challenge to explain how equal concentrations of cholesterol bathing the endothelium can produce local rather than global effects on arteries. As there are numerous reproducible sites that are prone to developing atherosclerosis (Malek *et al.* 1999; VanderLaan *et al.* 2004), a localizing element should be operating. The focal distribution of atherosclerotic lesions has been considered to be dependent, at least in part, on hydrodynamic factors. Previous study using a model of abdominal aorta stenosis with a U-shaped clip, showed deposits of lipids, as revealed by *in vivo* staining with Oil red O injected directly into the circulation, immediately upstream to the throat of the stenosis, related to high shear stress, and immediately downstream to the throat of the stenosis, related to low shear stress (Zand *et al.* 1991).

The present study was carried out to further test the hypothesis that haemodynamic forces are an important localizing factor that primes the local vascular wall in rats feeding a hypercholesterolaemic diet and submitted to infradiaphragmatic aortic constriction. These animals developed a normotensive prestenotic region with laminar blood flow and normal wall shear stress (WSS) that served as control for a normotensive poststenotic region with turbulent blood flow and low WSS.

Materials and methods

Experimental protocol

Hypercholesterolaemia was induced in male rats, weighing 156.10 ± 1.14 g, feeding a standard diet supplemented with 4% cholesterol (Dolder AG, Basel, Switzerland), 1% cholic acid (Sigma Chemical CO., St Louis, MO, USA), and 0.5% 2-thiouracil (Sigma) (Burstein *et al.* 1997). This hypercholesterolaemic diet started to be offered 2 days before surgery. The animals submitted to surgical abdominal aorta stenosis consumed the hypercholesterolaemic diet for more than 28 days. The Committee on Animal Research of the University of São Paulo approved all protocols.

Animal surgery

The animals were anaesthetized with ether and the abdominal aorta constricted just below the diaphragm as previously described (Rossi & Peres 1992). Briefly, the aorta was exposed through a left flank incision and a 0.94 mm diameter probe in L was placed next to the vessel. The aorta was constricted with a ligature of cotton thread around the probe tip, which was immediately removed, thus reducing the vessel lumen to the diameter of the probe. This experimental model was previously used in our laboratory to produce alteration of blood flow in the poststenotic aorta segment (Prado & Rossi 2006; Prado *et al.* 2006).

Harvesting and preparation of aortas for high resolution light microscopy

After 28 days, the aortas were rapidly excised from the trunk down to the iliac bifurcation, washed at a pressure-perfusion of 100 mmHg with phosphate-buffered saline (PBS) through the ascending aorta and followed by perfusion-fixation with phosphate-buffered 10% formalin for 1–2 min and then immersed non-pressurized in the same fixative for 24 h at room temperature. After fixation, the adventitial tissue was removed and the aortic tubes proximal and distal to the stenosis were transversally cut into 5–6 mm long segments. The samples were then dehydrated, embedded in Historesin (Leica Instruments, Heidelberg, Germany), serially cut at 2 μm, stained with toluidine blue, and examined in a light microscope.

Cross sections ($n = 9$), exactly perpendicular to the long axis of the aorta from each vascular segment, were morphometrically evaluated at magnification ×400. The absolute thickness of the intima and media, the cross-sectional area of the lumen and the perimeter in both prestenotic and poststenotic segments were measured as previously described (Rossi & Colombini-Netto 2001; Prado *et al.* 2006). Measurements were made by a skilled observer blinded to the treatment groups. The diameter was calculated according to the formula $d = 2\sqrt{a/\pi}$, where a is area of the aorta lumen expressed in mm^2 and π is 3.14. Morphometric analysis was performed using videomicroscopy with the LEICA QWIN software (Leica Imaging Systems Ltd, Cambridge, UK) in conjunction with a Leica microscope (Leica DMR; Leica

Microsystems Wetzlar GmbH, Wetzlar, Germany), videocamera (Leica DFC300FX; Leica Microsystems AG, Heerbrugg, Switzerland), and an on-line computer.

Immunohistochemistry

For immunohistochemical staining, aortas (n = 6) were harvested as above and embedded in paraffin. Immunolabelling was done in triplicate and performed for 3-nitrotyrosine (1:100; Upstate, Lake Placid, NY, USA). Sections 5 μm thick were placed on silane-coated slides, deparaffinized, washed in PBS, and then submitted to heat-induced antigen, endogenous peroxidase inhibition, and non-specific antibody binding block. After, the sections were incubated with the primary antibody. Antigen was visualized with a labelled streptavidin biotin peroxidase technique (Vectastain ABC kit; Vector Laboratories, Burlingame, CA, USA) with diaminobenzidine (DAB) substrate. Sections were then counterstained with haematoxylin, coverslipped, and examined by two skilled blinded observers. The effect of a standard chow diet and the hypercholesterolaemic diet on the 3-nitrotyrosine expression in the non-constricted infra-diaphragmatic aortas of rats was also evaluated. The immunoreactivity intensity and extension was graded in a semi-quantitative arbitrary scale 0 to 3: 0, no reaction; 1, mild reaction; 2, moderate reaction and 3, strong reaction.

Transmission electron microscopy (TEM)

The aortas (n = 4) were excised as described for high resolution light microscopy. After fixation with 2.5% glutaraldehyde in cacodylate buffer (pH 7.3) for 2 h and postfixation with osmium tetroxide for 2 h, the aortic tubes proximal and distal to the stenosis were dehydrated in ascending concentrations of acetone, and, subsequently, embedded in Araldite® (Polysciences, Warrigton, PA, USA). Ultrathin sections were obtained from selected areas with a diamond knife in a Sorvall MT-5000 ultramicrotome (DuPont Co., Wilmington, DE, USA), double-stained with uranyl acetate and lead citrate, and examined in a Zeiss EM109 electron microscope (Carl Zeiss, Oberköchen, Germany) at 80 kV.

Doppler

Aorta duplex ultrasonography (n = 6) under ether anaesthesia was performed 4 weeks after surgery using an Acuson Aspen apparatus (Acuson Corp., Mountain View, CA, USA) equipped with color Doppler facility and multi-frequency linear electronic transducer at 11 MHz. The rats were lying in the supine position. The aorta was visualized by ultrasonography. Doppler was performed in the region of stenosis, upstream and downstream.

Wall shear stress was calculated using the Poiseuille formula: $\tau = 4\eta BFR/\pi(kr)^3$, where τ is WSS (dyne/cm^2), η is the blood viscosity (0.03 poise), BFR is blood flow rate (ml/min), π is 3.14, k is 1.25 (the shrinkage index, which is the ratio of artery diameter before and after plastic embedding), and r is the arterial radius (cm).

Blood pressure

To assess the mean arterial blood pressures proximal and distal to the aortic constriction in anaesthetized animals (ketamine 74 mg/kg i.p. and xylazine 8 mg/kg i.p.), carotid and femoral pressures, respectively, were obtained 24 h and 14 and 28 days after surgery (n = 7 each day). With the animals under anaesthesia, a polyethylene catheter (PE-10) filled with heparinized saline was introduced and positioned either in the carotid artery and exteriorized in the neck or in the femoral artery and exteriorized in the groin. Immediately after surgical preparation, when haemodynamic was stable, mean carotid and femoral pressures were recorded by connecting the catheter to a PE-50 polyethylene catheter connected to the pressure transducer Powerlab (ADInstruments, Castle Hill, NSW, Australia). The mean carotid and femoral blood pressures of anaesthetized animals weighing 150 g and receiving hypercholesterolaemic diet for 2 days were also measured, simulating the time 0 of the experiment immediately before surgery.

Blood analysis

The serum concentration of total cholesterol was measured before and 4 weeks after the hypercholesterolaemic diet (n = 10 each day) by a spectrophotometric method using a commercially available kit (Cobas Mira; Roche Diagnostics, Basel, Switzerland).

Statistical analysis

Data were analysed using a GRAPHPAD PRISM statistic program (GraphPad Software Inc., San Diego, CA, USA). For analysis of differences between the prestenotic and poststenotic segments, Student's t-test was performed. Comparison of immunoreactivity intensity grade of 3-nitrotyrosine was made with the Kruskal–Wallis and Dunn's multiple comparison tests. A level of significance of 5% was chosen to denote differences between means. Unless specified, data are presented as mean ± standard error.

Results

Cholesterol level

The mean total serum cholesterol level at the beginning of the experiment was 62.63 ± 4.73 mg/dl. After 4 weeks, the level was markedly higher, 554.70 ± 64.78 mg/dl (mean ± standard deviation).

Blood pressure

The mean carotid and femoral blood pressure under hypercholesterolaemic diet were 96.00 ± 1.73 and 94.00 ± 1.78 mmHg before surgery of abdominal aorta constriction (day 0) respectively. After 24 h of surgery, the femoral blood pressure decreased 9.34% (89.00 ± 1.57 mmHg) in comparison with values in carotid blood pressure (98.17 ± 0.98 mmHg) ($P < 0.001$). The carotid and femoral blood pressures at day 14 (98.60 ± 3.52 and 94.20 ± 1.91 mmHg respectively) and at the end of the experiment (day 28) (96.83 ± 1.54 and 95.20 ± 0.66 mmHg respectively) were similar (Figure 1).

Doppler

Four weeks after surgery, the blood flow rate in the prestenotic segment was 48.12 ± 3.62 ml/min and in the poststenotic segment was markedly lower, 20.22 ± 2.47 ml/min (Figure 2a).

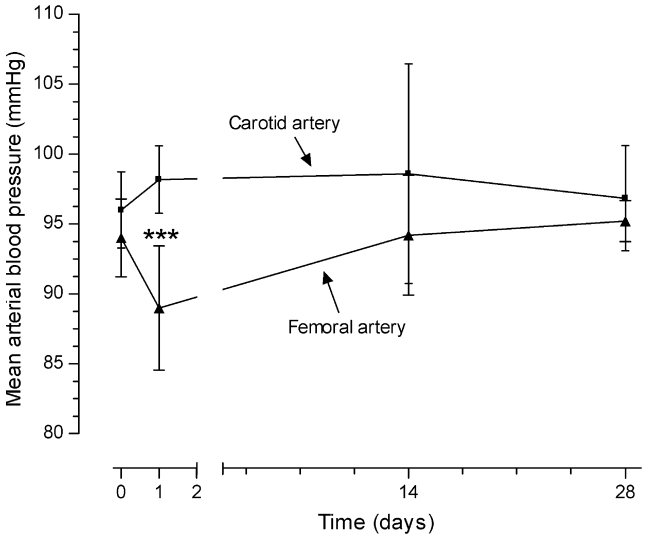

Figure 1 Mean carotid and femoral blood pressure of animals ($n = 7$ each day) submitted to surgical abdominal aorta stenosis and feeding hypercholesterolaemic diet during the 28-day period of study. ***$P < 0.001$.

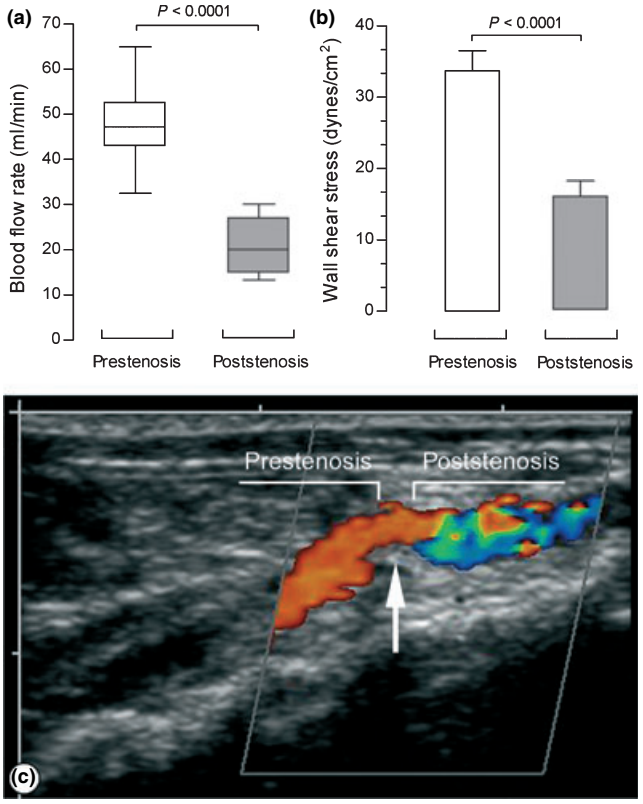

Figure 2 (a) Blood flow rate (ml/min). Box and whisker plot graph shows the batches of data in prestenotic and poststenotic aortas at day 28 of the experiment. (b) Wall shear stress mean values (dyne/cm^2) in prestenotic and poststenotic aortas at day 28 of the experiment ($n = 6$). (c) Color Doppler shows a laminar flow in the prestenotic segment characterized by orange-red colour. In the poststenotic segment, a mixed of orange-red and blue colour was seen characterizing turbulent blood flow.

The WSS value in the prestenotic segment was 33.72 ± 2.80 dyne/cm^2 and in the poststenotic segment was markedly lowered 15.91 ± 2.15 dyne/cm^2 (Figure 2b).

Color Doppler in the prestenotic segment could demonstrate a preserved laminar flow and the orange-red colour near the aorta wall meaning slower rate of laminar flow. In the poststenotic segment, a mixed of orange-red and blue was seen characterizing turbulent flow (Figure 2c).

High resolution light microscopy

The gross examination revealed that both prestenotic and poststenotic segments were similar. The use of plastic embedding allowed 2 μm thick sections with good resolution of structural details to be examined. The light microscopic study of the prestenotic segment revealed diffusely distributed foci of small flat lesions corresponding microscopically

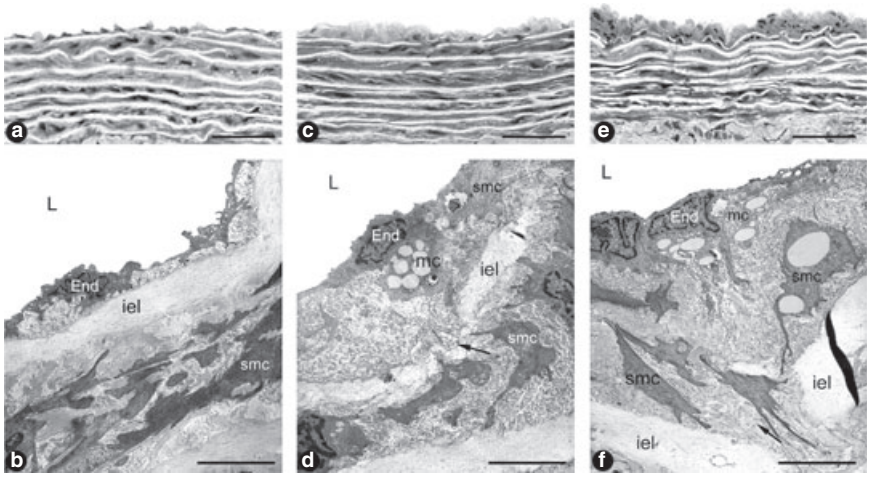

Figure 3 Panels A and B show representative aspects of the prestenotic and poststenotic aorta with high resolution light microscopy (a) (n = 9) and transmission electron microscopy (b) (n = 4). The appearance did not differ from that reported for mammalian aorta. Panels C and D show representative views of the prestenotic small flat lesions corresponding to fatty streaks characterized by intimal foam cells accumulation with high resolution light microscopy (c) and a few vacuolated mononuclear and smooth muscle cells with transmission electron microscopy (d). Panels E and F show representative views of the poststenotic raised incipient atherosclerotic lesions composed of mononuclear and smooth muscle cells, many of them vacuolated, with high resolution light microscopy (e) and vacuolated mononuclear cells and a great number of vacuolated smooth muscle cells surrounded by extracellular matrix with transmission electron microscopy (f). End, endothelial cell; iel, internal elastic lamina; smc, smooth muscle cell; mc, mononuclear cell; arrow, migration of smooth muscle cell from the media to the intima. In a, c and e, bar magnification=20 μm; in b, d and f, bar magnification=5 μm.

to fatty streaks characterized by intimal foam cells accumulation (Figure 3c) contrasting with the delicate dominant structure of the intima in most of the aorta wall (Figure 3a). In contrast, in the poststenotic segment focally distributed incipient atherosclerotic lesions characterized by raised focal lesions within the intima composed of smooth muscle cells, mononuclear cells and extracellular matrix were seen (Figure 3e). The remaining intima of the poststenotic segment appeared delicate similar to that observed in the prestenotic segment.

Transmission electron microscopy

In the prestenotic and poststenotic segments most of the intima appeared no different from that reported for mammalian aorta (Figure 3b), except for the focal lesions referred above. The small flat lesions observed in the prestenotic segment, corresponding to fatty streaks at the high resolution light microscopic study, were composed of mononuclear and smooth muscle cells with vacuolated cytoplasm surrounded by collagen matrix localized in the subendothelial space (Figure 3d). Smooth muscle cells migrating from the media into the intima could also be seen (Figure 3d,f). In the poststenotic segment, the incipient atherosclerotic lesions at the high resolution light microscopy study were composed by vacuolated mononuclear cells and great number of smooth muscle cells, many of then vacuolated surrounded by collagen matrix (Figure 3f).

Morphometry

The constriction of the abdominal aorta resulted in a mean reduction of 80% of the luminal infra-diaphragmatic aorta. Grossly no poststenotic dilatation was seen at the end of the experiment.

Table 1 shows the data of the intima and media thicknesses, luminal area, perimeter, diameter, WSS and blood flow rate of the prestenotic and poststenotic aorta segments.

When the percentile frequency distribution of intima thickness in the prestenotic segment was plotted, the small flat lesions can be evidenced. The percentile frequency distribution of intima thickness in the poststenotic segment can clearly demonstrate the occurrence of marked intimal thickening, corresponding to the incipient atherosclerotic lesions absent in the prestenotic segment (Figure 4).

Immunohistochemistry

The immunohistochemical analysis revealed an increased expression of 3-nitrotyrosine in endothelial and, mainly,

Table 1 Intima and media thickness, luminal area, perimeter, diameter (n = 9), blood flow rate and wall shear stress (n = 6) of the prestenosis and poststenosis segments of the infra-abdominal aorta submitted to constriction

	Prestenosis segment	Poststenosis segment
Intima thickness (μm)	6.99 ± 1.41	7.80 ± 1.61
Media thickness (μm)	94.81 ± 8.67	81.07 ± 9.01*
Luminal area (mm)	1.87 ± 0.30	1.69 ± 0.22
Perimeter (mm)	6.66 ± 0.44	6.26 ± 0.75
Diameter (mm)	1.53 ± 0.13	1.46 ± 0.10
Blood flow rate (ml/min)	48.12 ± 9.85	20.22 ± 6.05***
Wall shear stress (dyne/cm^2)	33.72 ± 7.91	15.91 ± 5.66**

Values are mean ± standard deviation.
*P < 0.05, **P < 0.001, ***P < 0.0001.

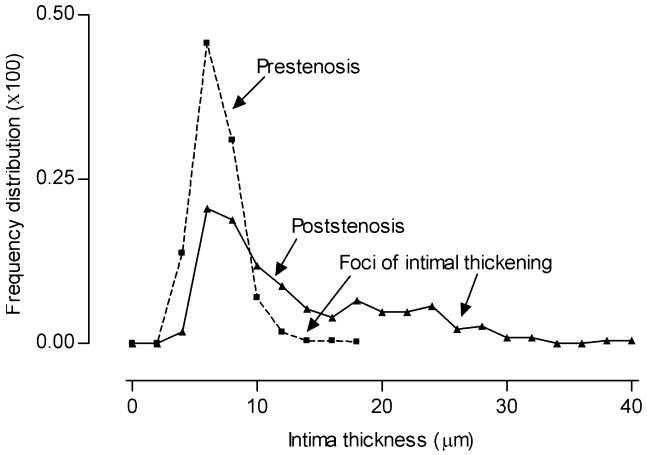

Figure 4 Percentile frequency distribution of intimal thickness. When the percentile frequency distribution of intima thickness in the prestenotic and poststenotic segments was plotted, the small flat lesions can be evidenced. The occurrence of marked intimal thickening, corresponding to the raised incipient atherosclerotic lesions, absent in the prestenotic segment, can be clearly demonstrated.

smooth muscle cells in the prestenotic (Figure 5c) and more markedly in the poststenotic segments (Figure 5d) of aortas from animals feeding hypercholesterolaemic diet in comparison with control aortas of animals feeding standard chow diet (Figure 5a). Non-constricted aortas from rats given the hypercholesterolaemic diet (Figure 5b) also showed an increased expression of 3-nitrotyrosine similar to that of the aorta prestenotic segment. Figure 5e shows the result of the semi-quantitative evaluation of 3-nitrotyrosine immunoreactivity intensity grade.

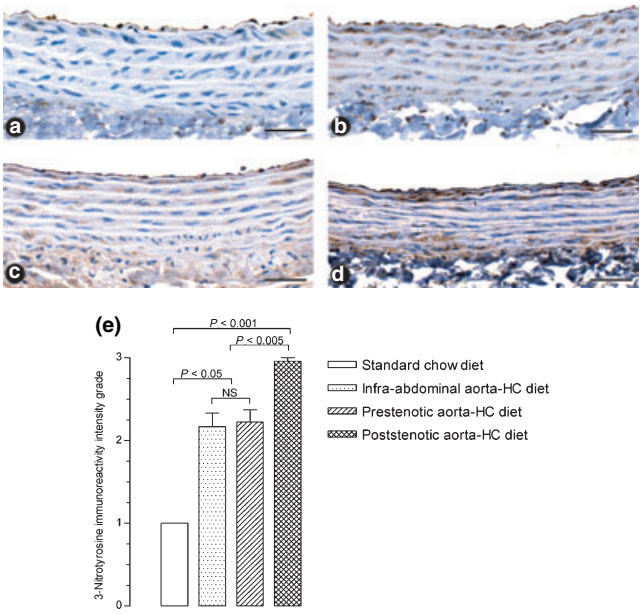

Figure 5 Immunohistochemistry (n = 6). The analysis revealed an increased expression (brown stained features) of 3-nitrotyrosine in endothelial and smooth muscle cells in the prestenotic (panel c) and more markedly in the poststenotic (panel d) segments of aortas from animals feeding hypercholesterolaemic diet. Aortas of animals feeding normal chow diet (panel a) show expression of 3-nitrotyrosine mainly in endothelial cells. Non-constricted aortas from rats given the hypercholesterolaemic diet also showed an increased expression of 3-nitrotyrosine (panel b) in endothelial and smooth muscle cells, comparable to that of the aorta prestenotic segment. Bar magnification=50 μm. The graph (panel e) shows the results of the semi-quantitative evaluation of 3-nitrotyrosine immunoreactivity intensity grade.

Discussion

It is well-known that diet-induced hyperlipidemia and atherosclerotic lesions develop more easily in some species than in others. Rats are generally considered to be resistant to naturally occurring and experimentally induced atherosclerosis (Vesselinovitch 1988; Moghadasian 2002). High doses of dietary cholesterol combined with bile acids and experimentally induced hypothyroidism has been demonstrated to help the development of atherosclerotic lesions in rats (Burstein *et al.* 1997), these extremes in dietary protocol being required to induce significant hypercholesterolaemia. In the present study, rats given a hypercholesterolaemic diet developed a nine times higher mean blood cholesterol level when compared with that of rats fed a standard rat chow diet. In addition, the abdominal aorta constriction associated with diet-induced hypercholesterolaemia produced a normotensive prestenotic segment with laminar blood flow and normal WSS and a normotensive poststenotic segment with

turbulent blood flow and low WSS. It has been demonstrated that this model of aorta constriction produces a hypertensive prestenotic segment and a normotensive poststenotic segment (Rossi & Peres 1992; Barton *et al.* 2001; Prado & Rossi 2006; Prado *et al.* 2006). The presence of normotension in aortic prestenotic segments in hypercholesterolaemic animals can be ascribed to the diet supplemented with thiouracil, which is known to induce hypothyroidism and hypotension in rats (Delia & Thompson 1988).

Hypercholesterolaemia has been extensively associated with endothelial cell dysfunction, considered a key early step in the atherogenic process (Dickhout *et al.* 2005), and consequent increased vascular production/release of superoxide anions (Ohara *et al.* 1993; Warnholtz *et al.* 1999). Because 3-nitrotyrosine was noted previously by immunohistochemistry in human atherosclerotic lesions (Luoma *et al.* 1998), 3-nitrotyrosine expression in both prestenotic and poststenotic was assessed. An increased presence of 3-nitrotyrosine in endothelial and smooth muscle cells was detected in the prestenotic and more markedly in the poststenotic aorta segments of rats given a hypercholesterolaemic diet in comparison with the 3-nitrotyrosine expression in the infra-diaphragmatic aorta from rats fed a standard chow diet. Control animals given the hypercholesterolaemic diet also showed an increased expression of 3-nitrotyrosine in endothelial and smooth muscle cells, comparable to that observed in the prestenotic segments. Hypercholesterolaemic diet has been demonstrated to strikingly increase the expression of 3-nitrotyrosine in endothelium, smooth muscle layers and adventitia of the aorta in rabbits (Adachi *et al.* 2002). The even more pronounced expression of 3-nitrotyrosine in the poststenotic segments is very likely due to an additional factor, haemodynamic alterations. This assumption is supported by recent study on human coronary arteries showing that 3-nitrotyrosine is present in arterial regions exposed to oscillatory shear stress (curvatures and bifurcations), but not in arterial regions exposed to pulsatile shear stress (straight segments) (Hsiai *et al.* 2007). The increased presence of 3-nitrotyrosine indicates an increased production of nitric oxide and superoxide anions that interact to produce peroxynitrite, a powerful oxidant causing damage to multiple cells constituents, including proteins (Koppenol *et al.* 1992). The accumulation of 3-nitrotyrosine, which is the footprint of nitric oxide oxidation/inactivation by reactive oxygen species, supports the supposition of endothelial cell dysfunction elicited by hypercholesterolaemia. Although nitrotyrosine is considered an emergent inflammatory marker for atherosclerosis (Shishehbor *et al.* 2003), the mechanism by which peroxynitrite formation contributes to atherogenesis remains uncertain.

Diffuse foci of small flat lesions corresponding to fatty streaks, contrasting with the dominant delicate structure of the intima in most of the aorta wall, were seen in the prestenotic segment. These small flat lesions could be evidenced when the percentile frequency distribution of intima thickness was plotted. Electron microscopically, vacuolated mononuclear and smooth muscle cells surrounded by scanty extracellular matrix could be evidenced. Laminar blood flow and normal WSS have been considered as atheroprotective (Dardik *et al.* 2005). The presence of these small flat lesions may be attributed to endothelial cell dysfunction related to hypercholesterolaemia and oxidative stress. In contrast, the poststenotic segment showed normal intima appearing delicate, similar to that observed in the prestenotic segment, except for focally distributed incipient atherosclerotic lesions characterized by raised intimal focal lesion composed of vacuolated mononuclear cells and a great number of vacuolated and non-vacuolated smooth muscle cells and extracellular matrix. These incipient atherosclerotic lesions, absent in the prestenotic segment, could be clearly demonstrated when the percentile frequency distribution of intima thickness was plotted. No qualitative morphologic alterations were observed in the media layer in both segments, except for its decreased mean thickness in the poststenotic segment, which can be due to variations in the wall thickness observed in the length of the aorta (Guo *et al.* 2002). It has been demonstrated that the haemodynamic environment, mainly shear stress and blood flow pattern, is a determinant of the susceptibility to the development of atherosclerotic lesions in branches, curvatures and bifurcations of elastic and muscular arteries (Davies 2000; Suo *et al.* 2007). Several mechanisms have been proposed from *in vitro* studies to account for the association between low WSS and the formation of local atheroma, including modulation of endothelial function and structure and regulation of endothelial gene expression (Malek & Izumo 1995; Resnick & Gimbrone 1995), modification of bulk transport of lipid (Fatouraee *et al.* 1998) and promotion of monocyte adhesion to the endothelial wall (Honda *et al.* 2001).

In summary, the present study clearly demonstrated that the combination of turbulent blood flow and low WSS in the presence of hypercholesterolaemia and oxidative stress creates conditions to the formation of focally distributed incipient atherosclerotic lesions observed in the poststenotic segment. In contrast, only diffuse fatty streaks could be observed in the normotensive prestenotic segment with laminar blood flow and normal WSS in the presence of hypercholesterolaemia and oxidative stress. In other words, turbulent blood flow plays an essential localizing role in plaque formation in experimentally induced hypercholesterolaemic

rats. Although haemodynamic forces are not by themselves responsible for the pathogenesis of atherosclerosis, they prime the local vascular wall in which the lesion develop. Further studies are required to establish how haemodynamic forces are detected and transduced into chemical signalling by the cells of the artery wall and then converted into pathophysiologically relevant phenotypic changes.

Acknowledgements

The authors thank Lígia B. Santoro, Maria E. Riul, Mônica A. Abreu, for excellent technical assistance. This study was supported by grants from the Fundação de Amparo à Pesquisa do Estado de São Paulo (FAPESP 01/09879-8, 06/52882-3, 06/59618-0), Conselho Nacional de Desenvolvimento Científico e Tecnológico and Coordenação de Aperfeiçoamento de Pessoal de Nível Superior (CAPES).

References

Adachi T., Matsui R., Xu S. *et al.* (2002) Antioxidant improves smooth muscle sarco/endoplasmic reticulum Ca2+-ATPase function and lowers tyrosine nitration in hypercholesterolemia and improves nitric oxide-induced relaxation. *Circ. Res.* **90**, 1114–1121.

Anderson K.M., Castelli W.P., Levy D. (1987) Cholesterol and mortality. 30 years of follow-up from the Framingham study. *JAMA* **257**, 2176–2180.

Anitschkow N. & Chalatow S. (1913) Über experimentelle cholesterinsteatose und ihre bedeutung für die entstehung einiger pathologischer prozesse. *Zentralbl. Allg. Pathol.* **24**, 1–9.

Assmann G., Cullen P., Schulte H. (2002) Simple scoring scheme for calculating the risk of acute coronary events based on the 10-year follow-up of the prospective cardiovascular Munster (PROCAM) study. *Circulation* **105**, 310–315.

Barton C.H., Ni Z., Vaziri N.D. (2001) Enhanced nitric oxide inactivation in aortic coarctation-induced hypertension. *Kidney Int.* **60**, 1083–1087.

Burstein P.J., Draznin B., Johnson C.J., Schalch D.S. (1997) The effect of hypothyroidism on growth, serum growth hormone, the growth hormone-dependent somatomedin, insulin-like growth factor, and its carrier protein in rats. *Endocrinology* **104**, 1107–1111.

Dardik A., Chen L., Frattini J. *et al.* (2005) Differential effects of orbital and laminar shear stress on endothelial cells. *J. Vasc. Surg.* **41**, 869–880.

Davies P.F. (2000) Spatial hemodynamics, the endothelium, and focal atherogenesis: a cell cycle link? *Circ. Res.* **86**, 114–116.

Delia A.J. & Thompson E.B. (1988) A time-course study of hypothyroidism-induced hypotension: its relation to food deprivation. *Arch. Int. Pharmacodyn. Ther.* **296**, 210–223.

Dickhout J.G., Hossain G.S., Pozza L.M., Zhou J., Lhoták S., Austin R.C. (2005) Peroxynitrite causes endoplasmic reticulum stress and apoptosis in human vascular endothelium: implications in atherogenesis. *Arterioscler. Thromb. Vasc. Biol.* **25**, 2623–2629.

Fatouraee N., Deng X., De Champlain A., Guidoin R. (1998) Concentration polarization of low density lipoproteins (LDL) in the arterial system. *Ann. N. Y. Acad. Sci.* **858**, 137–146.

Grundy S.M., Cleeman J.I., Merz C.N. *et al.* (2004) American College of Cardiology Foundation; American Heart Association. Implications of recent clinical trials for the National Cholesterol Education Program Adult Treatment Panel III guidelines. *Circulation* **110**, 227–239.

Guo X., Kono Y., Mattrey R., Kassab G.S. (2002) Morphometry and strain distribution of the C57BL/6 mouse aorta. *Am. J. Physiol. Heart Circ. Physiol.* **283**, H1829–H1837.

Hartvigsen K., Binder C.J., Hansen L.F. *et al.* (2007) A diet-induced hypercholesterolemic murine model to study atherogenesis without obesity and metabolic syndrome. *Arterioscler. Thromb. Vasc. Biol.* **27**, 878–885.

Honda H.M., Hsiai T., Wortham C.M. *et al.* (2001) A complex flow pattern of low shear stress and flow reversal promotes monocyte binding to endothelial cells. *Atherosclerosis* **158**, 385–390.

Hsiai T.K., Hwang J., Barr M.L. *et al.* (2007) Hemodynamics influences vascular peroxynitrite formation: implication for low-density lipoprotein apo-B-100 nitration. *Free Radic. Biol. Med.* **42**, 519–529.

Klag M.J., Ford D.E., Mead L.A. *et al.* (1993) Serum cholesterol in young men and subsequent cardiovascular disease. *N. Engl. J. Med.* **328**, 313–318.

Koppenol W.H., Moreno J.J., Pryor W.A., Ischiropoulos H., Beckman J.S. (1992) Peroxynitrite, a cloaked oxidant formed by nitric oxide and superoxide. *Chem. Res. Toxicol.* **5**, 834–842.

Lichtman A.H., Clinton S.K., Iiyama K., Connelly P.W., Libby P., Cybulsky M.I. (1999) Hyperlipidemia and atherosclerotic lesion development in LDL receptor-deficient mice fed defined semipurified diets with and without cholate. *Arterioscler. Thromb. Vasc. Biol.* **19**, 1938–1944.

Luoma J.S., Strålin P., Marklund S.L., Hiltunen T.P., Särkioja T., Ylä-Herttuala S. (1998) Expression of extracellular SOD and iNOS in macrophages and smooth muscle cells in human and rabbit atherosclerotic lesions: colocalization with epitopes characteristic of oxidized LDL and peroxynitrite-modified proteins. *Arterioscler. Thromb. Vasc. Biol.* **18**, 157–167.

Malek A.M. & Izumo S. (1995) Control of endothelial cell gene expression by flow. *J. Biomech.* **28**, 1515–1528.

Malek A.M., Alper S.L., Izumo S. (1999) Hemodynamic shear stress and its role in atherosclerosis. *JAMA* **282**, 2035–2042.

Moghadasian M.H. (2002) Experimental atherosclerosis: a historical overview. *Life Sci.* **70**, 855–865.

Ohara Y., Peterson T.E., Harrison D.G. (1993) Hypercholesterolemia increases endothelial superoxide anion production. *J. Clin. Invest.* **91**, 2546–2551.

Prado C.M. & Rossi M.A. (2006) Circumferential wall tension due to hypertension plays a pivotal role in aorta remodelling. *Int. J. Exp. Pathol.* **87**, 425–436.

Prado C.M., Ramos S.G., Alves-Filho J.C., Elias J. Jr, Cunha F.Q., Rossi M.A. (2006) Turbulent flow/low wall shear stress and stretch differentially affect aorta remodeling in rats. *J. Hypertens.* **24**, 503–515.

Resnick N. & Gimbrone M.A. Jr (1995) Hemodynamic forces are complex regulators of endothelial gene expression. *FASEB J.* **9**, 874–882.

Ross R. (1986) The pathogenesis of atherosclerosis-an update. *N. Engl. J. Med.* **314**, 488–500.

Rossi M.A. & Colombini-Netto M. (2001) Chronic inhibition of NO synthesis per se promotes structural intimal remodeling of the rat aorta. *J. Hypertens.* **19**, 1567–1579.

Rossi M.A. & Peres L.C. (1992) Effect of captopril on the prevention and regression of myocardial cell hypertrophy and interstitial fibrosis in pressure overload cardiac hypertrophy. *Am. Heart J.* **134**, 700–709.

Shishehbor M.H., Aviles R.J., Brennan M.L. *et al.* (2003) Association of nitrotyrosine levels with cardiovascular disease and modulation by statin therapy. *JAMA* **289**, 1675–1680.

Steinberg D., Parthasarathy S., Carew T.E., Khoo J.C., Witztum J.L. (1989) Beyond cholesterol. Modifications of low-density lipoprotein that increase its atherogenicity. *N. Engl. J. Med.* **320**, 915–924.

Suo J., Ferrara D.E., Sorescu D., Guldberg R.E., Taylor W.R., Giddens D.P. (2007) Hemodynamic shear stresses in mouse aortas: implications for atherogenesis. *Arterioscler. Thromb. Vasc. Biol.* **27**, 346–351.

VanderLaan P.A., Reardon C.A., Getz G.S. (2004) Site specificity of atherosclerosis: site-selective responses to atherosclerotic modulators. *Arterioscler. Thromb. Vasc. Biol.* **24**, 12–22.

Vesselinovitch D. (1988) Animal models and the study of atherosclerosis. *Arch. Pathol. Lab. Med.* **112**, 1011–1017.

Warnholtz A., Nickenig G., Schulz E. *et al.* (1999) Increased NADH-oxidase-mediated superoxide production in the early stages of atherosclerosis: evidence for involvement of the renin-angiotensin system. *Circulation* **99**, 2027–2033.

Zand T., Majno G., Nunnari J.J. *et al.* (1991) Lipid deposition and intimal stress and strain. A study in rats with aortic stenosis. *Am. J. Pathol.* **139**, 101–113.